Supporting Information – Appendix

Capture of micrococcin biosynthetic intermediates reveals C-terminal processing as an obligatory step for *in vivo* maturation

Kathryn D. Bewley[a,1], Philip R. Bennallack[b,1], Mark A. Burlingame[a], Richard A. Robison[b], Joel S. Griffitts[b], and Susan M. Miller[a,2]

[a]Department of Pharmaceutical Chemistry, University of California-San Francisco, San Francisco, CA 94158; [b]Department of Microbiology and Molecular Biology, Brigham Young University, Provo, UT 84602; [1]K.D.B and P.R.B contributed equally to this work. [2]Correspondence should be addressed to Susan Miller, Susan.MillerPhd@ucsf.edu

SI Materials and Methods

Construction, expression and purification of *E. coli*-produced GST-TclE

To optimize conditions for expression and analysis of the precursor peptide (TclE), a GST-TclE translational fusion was created by overlap-extension PCR and introduced into the high copy *E. coli* expression vector (pJG542) under control of an IPTG-inducible promoter. The glutathione S-transferase (GST) encoding gene was sourced from pGEX-4T-1 (GE Life Sciences, Marlborough, MA, USA) and amplified using oPB281 and oPB288 (Table S2). The *tclE* gene was amplified from pBac115 (1) using oPB282 and oPB289. Once assembled and the sequence verified, expression of GST-TclE was achieved by transforming the construct into Rosetta 2(DE3) pLysS cells (EMD Biosciences), inoculating a single colony into a 25 mL overnight culture (LB media, 37 °C, carbenicillin 100 mg/L and chloramphenicol 34 mg/L) followed by inoculation into a 1-L fermentation flask (LB media, 37 °C, carbenicillin 100 mg/L and chloramphenicol 34 mg/L). Cells were grown until the OD_{600} = 0.6-0.65 upon which 0.25 mM IPTG was added to induce expression for 3 hours at 37 °C. The cells were then pelleted, and GST-TclE was purified as described for GST-TclE peptides isolated from *B. subtilis* mutant strains.

Purification of processed peptide intermediates.

For each *B. subtilis tcl* mutant or deletion strain, a single colony was grown overnight in LB medium (25 ml, 37 °C, 200 rpm) with spectinomycin (80 mg/L). This was used to inoculate LB medium (1 L, 37 °C, 200 rpm, 16 h or 8 h) with spectinomycin (80 mg/L) and xylose (1%) to induce production of the biosynthetic enzymes. Cells were harvested by centrifugation for 15 min at 7,878 × g. Cell pellets were frozen for later use. Thawed pellets were resuspended in 50 mM sodium phosphate buffer with 100 mM NaCl, pH 7.5 (NaPiCl). DNase and a protease inhibitor tablet (Roche) were added, and the cells were sonicated for 2 min (duty cycle, 50%; output, 6) on ice using a Branson Sonifier 450, followed by centrifugation for 20 min at 32,539 × g. The clarified supernatant was incubated with glutathione resin (1 mL of resin per liter of culture) for 30 min with gentle shaking at room temperature. The slurry was collected by centrifugation for 5 min at 700 × g. The resin was washed with 3 × 10 mL of NaPiCl, centrifuging after each wash. To elute the GST-peptide, the resin was incubated with 4 × 1 mL of 50 mM Tris HCl, pH 8 with 10 mM reduced glutathione for 10 min at room temperature before centrifuging. The combined 4 mL of elution supernatant was syringe filtered to remove any remaining resin beads and was then concentrated using a 10 kDa MW cutoff Amicon spin filter (2,600 × g). The concentrated GST-peptide was buffer exchanged into 10 mM NaPi, pH 7.5 buffer using the same Amicon spin filter, concentrated to <100 μL, aliquoted and frozen at –80 °C. For ΔTclM strains only,

tobacco etch virus (TEV) protease cleavage of the peptide was carried out on the resin. To do this, 20 μg of TEV protease in 1 mL of NaPiCl containing 0.5 mM dithiothreitol (DTT) was added and incubated at room temperature for 1 h. The resin was centrifuged and supernatant was collected. The resin was washed with 2 × 1 mL of NaPiCl without DTT or protease. The 3 mL were combined, filtered and concentrated to <100 μL with a 3 kDa MW cutoff Amicon spin filter, aliquoted and frozen at –80 °C.

Alignments and Data Analysis

The structural alignments generated by HHpred are displayed in this Appendix using JalView (2). The structural models from Modeller were overlaid with their template structures using Chimera (3) and its MatchMaker feature, but ultimately illustrated in this Appendix using Pymol (PyMOL Molecular Graphics System, Version 1.7.4.1 Schrödinger, LLC.). The alignment of TclM and its homologues was generated with Clustal Omega (4) and displayed using JalView. Deconvolution of ESI-MS data was achieved with MagTran (The Magic Transformer), a software package based on the Zscore algorithm (5).

Fig. S1. Comparison of Tcl proteins from *M. caseolyticus* 115 and *B. cereus* ATCC 14579. (*A*) Alignment of TclE precursor peptides from *B. cereus* and *M. caseolyticus*. The core peptide is shown in red, and the leader peptide is shown in black. (*B*) The predicted functions of micrococcin biosynthetic proteins from *B. cereus* (*Bc*) and *M. caseolyticus* (*Mc*).

A

```
B. cereus ATCC 14579:     MGSEIKKALNTLEIEDFDAIEMVDVDAMPENEALEIMGASCTTCVCTCSCCTT
M. caseolyticus str. 115:   MGSEFQTNNIEGLDVTDLEFISEEVTEKDEKEIMGASCTTCVCTCSCCTT
```

B

Mc Gene Product (size, aa, GenBank ID)	*Bc* Gene Product (size, aa, GenBank ID)	Predicted function	Identity/similarity/ coverage %[a]
TclI (242) AIU53944.1	TclI (503) AAP11955.1	Ocin-ThiF-like protein	36/45/23
TclJ (563) AIU53945.1	TclJ (660) WP_001031656.1[b]	TOMM cyclodehydratase	35/50/87
TclK (843) AIU53946.1	TclK (871) AAP11953.1	dehydratase	28/47/92
TclL (267) AIU53947.1	TclL (323) AAP11952.1	dehydratase	28/45/95
TclM (264) AIU53948.1	TclM (325) AAP11951.1	aza-Diels-Alderase	32/52/79
TclN (447) AIU53949.1	TclN (522) AAP11950.1	McbC-type dehydrogenase	25/43/95
TclP (232) AIU53950.1	TclP (256) AAP11948.1	Short-chain dehydrogenase	38/57/99
TclS (223) AIU53941.1	TclS (237) AAP11945.1	Short-chain dehydrogenase	23/44/81

[a] Identity, similarity and coverage % numbers are based on a blastp comparison of *B. cereus* ATCC 14579 and *M. caseolyticus* str. 115 *tcl* gene products.

[b] There is some discrepancy in the length of *Bc*TclJ. It was originally deposited as BC5085 (547 aa), but it was later determined this was an N-terminal truncation and *Bc*TclJ is actually longer (660 aa). The 547 aa version has the GenBank ID AAP11954.1, while the 660 aa version has GenBank ID WP_001031656.1.

Fig. S2. Integration plasmids and GST-TclE precursor peptide gene/protein sequences. (*A*) Plasmid map of pLEGO harboring the biosynthetic genes (*tcl*IJKLMNPS) for expression with a xylose-inducible promoter after integration into the *amyE* locus of *B. subtilis* (6). (*B*) Plasmid map of pTclE_GST, for *thrC* integration and constitutive expression of the precursor peptide, TclE. A TEV-cleavage site was engineered between the N-terminal GST tag and TclE. (*C*) DNA sequence of the TEV-TclE portion of GST-TclE (spacer regions = lower case, TEV recognition site = underlined yellow highlight, TclE = grey highlight) and the resulting peptide after TEV cleavage (core peptide = underlined). The sequence of the untagged precursor peptide (TclE) is shown for comparison.

A

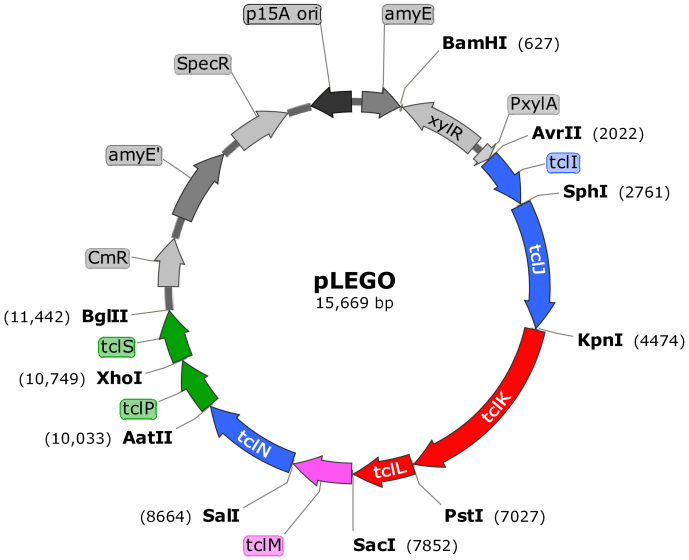

B

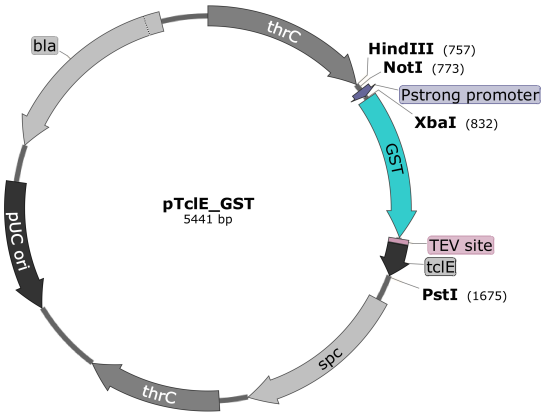

C

```
---Glutathione-S-transferase---ggaggaGAAAACCTGTATTTTCAAGGCggaTCAGAATTCCAAACAAACAATA
TCGAAGGTTTAGATGTCACTGATTTAGAATTTATCAGTGAAGAAGTTACTGAAAAAGACGAGAAAGAAATCATGGGTGCTTCT
TGTACTACATGTGTTTGTACATGCAGTTGTTGTACAACTTAA

GST-TclE Post TEV cleavage: GGSEFQTNNIEGLDVTDLEFISEEVTEKDEKEIMGASCTTCVCTCSCCTT
Untagged TclE:                MSEFQTNNIEGLDVTDLEFISEEVTEKDEKEIMGASCTTCVCTCSCCTT
```

Fig. S3. TclJ alignment and structural model. (*A*) TclJ is predicted to have a structure similar to ~450 residues of the C-terminus of LynD (PDB: 4V1T). The HHpred alignment of TclJ and LynD (probability >99%) identifies two conserved sequences involved in Mg^{2+} binding in the active site of LynD (LynD numbering): 423 EAXER 427, 548 EXXER 552; as well as a conserved C-terminus (572 PXPF 575) that also lies in the active site (7). The red asterisk (*) shows the predicted Mg-binding residue in TclJ (E319) mutated in this study. (*B*) Overlay of the Modeller structure of TclJ (magenta) derived from the HHpred alignment with LynD (cyan). Residues 107-562 of TclJ comprise the predicted globular domain with the catalytic active site. The disparate size and large gaps in sequences between the N-termini of the two proteins gives less confidence in the predicted structure of the ~100 N-terminal residues of TclJ. (*C*) Close up of the ATP binding site in LynD (cyan) overlaid with TclJ (magenta): ADP (green), phosphate (orange), Mg^{2+} (grey spheres), and E548/E319 (cyan/magenta) (7). E548/E319 is from one of the two conserved EXXER motifs, which have been shown to coordinate Mg^{2+} in the homologous BalhD protein (8).

A

```
TclJ    4 FESPEFNIIRYLSNSYI--FK-STSKEPDFLNSIKERILLNTN----------------------43
4V1T  174 LESQQTWLLVKPVGSVLWLGPVFVPGKTGCWDCLAHRLRGNREVEASVLRQKQAQQQRNGQSGSV 238

TclJ   44 -----DIIYKKNIPERNISFLSRIENSIGNFIC----NQI----------SEYDYIIYIYNHKT 88
4V1T  239 IGCLPTAR------ATLPSTLQTGLQFAATEIAKWIVKYHVNATAPGTVFFPTLDGKIITLNHSI 297

TclJ   89 NKIKKVNYFISPHYYKK-LPND---TTNCFNIIINELKN--SKSHNFRSRNIDSIYNQLDKYFLD 147
4V1T  298 LDLKSHILIKRSQCPTCGDPKILQHRGFEPLKLESRPKQFTSDG-GHRGTTPEQTVQKY-QHLIS 360

TclJ  148 KNLGICNMLLDNYD--G-PFPISVAMLPLDN---------GKEEPGVGRTRKIQRSRAVALLEAY 200
4V1T  361 PVTGVVTELVRITDPANPLVHTYRAGHSFGSATSLRGLRNTLKHKSSGKGKTDSQSKASGLCEAV 425

TclJ  201 ERYSGLEPRGKKTINHTE--DLKSKKVNMNSLILHNNPFLISHGIKN---------SNFTY--ND 252
4V1T  426 ERYSGIFQGD-EPRKRATLAELGDLAIHPEQCLCFSDG-----QYANRETLNEQATVAHDWIPQR 484

TclJ  253 -LLDNEISWVKCLNLNTFQTLLIPEQYAYYGINISNHKEKAINIAYEISNGCSVGNNYLEVVYYG 316
4V1T  485 FDASQAIEWTPVWSLTEQTHKYLPTALCYYHYPLP----PEHRFARGDSNGNAAGNTLEEAILQG 545
                *
TclJ  317 LMEVIERDSFLCSWYFNTPKDKISLKNASTSIKNLIQQFTSYYNDYKLELFYLYNEFNIPVVLAT 381
4V1T  546 FMELVERDGVALWWYNRLRRPAVDLGSFNEPYFVQLQQFYR-ENDRDLWVLDLTADLGIPAFAGV 609

TclJ  382 VTLKESSTKKMNFMCAAAADINIEDAIEKSIHEIGGILFGLNKKFIDRYHELEAIRKNNLDVKTM 446
4V1T  610 SNRKTG--SSERLILGFGAHLDPTIAILRAVTEVNQIGLELDKVPDE---NLKSDATDWLITEKL 669

TclJ  447 EDHTLVYGLPEHRTYIQQKMNYENIYDYDKEL--TPKIFYKEVQKLIKKI-STTKDILLVDQTPL 508
4V1T  670 ADHPYLLPDT----------TQPLKTAQDYPKRWSDDIYTDVMTCVNIAQQAGLETLVIDQTRP 723

TclJ  509 ISKKIDLKVGKIIVPGLLPMTFGKYNIRVSENRY-----HELCHFY-S-KDLIIDLNPHPF    562
4V1T  724 DI---GLNVVKVTVPGMRHFWSR------FGEGRLYDVPVKLGWLDEPLTEAQMNPTPMPF    775
```

B

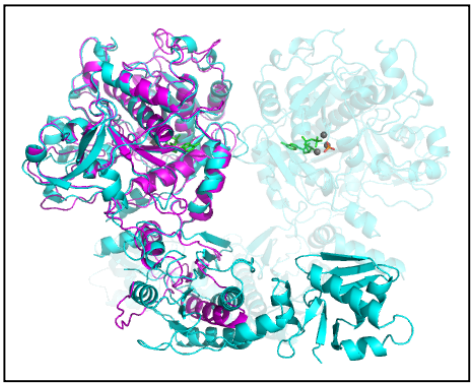

C

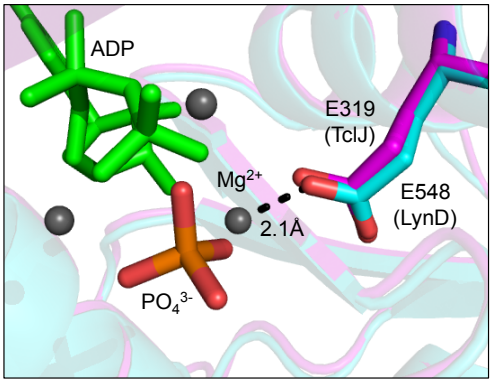

Fig. S4. TclK structural modeling and expanded mass spectrometry data for modified TclE from the TclK-defective strain. (*A*) HHpred alignment of TclK with N-terminal domain of NisB (probability >99%). Based on inactivation of NisB by an R83A mutation (9), we mutated conserved R181 to alanine for this study (*). Other residues identified in NisB as important for glutamylation of the NisA peptide are labeled (*) (9). (*B, left*) Overlay of TclK model (magenta, from HHpred alignment and Modeller) with NisB dimer (PDB: 4WD9, C-terminus = cyan, N-terminus = green). Most of the TclK model aligns well, but several loop regions differ. (*B, right*) Closeup of TclK model (magenta) with active site of NisB (green) showing aligned residues that are important for glutamylation activity. (*C*) We observed a degradation product in most samples prepared for mass spectrometry (peak 1 in MALDI and peaks a & d in ESI). The *m/z* of the MALDI-MS peak is consistent with a peptide with the same modifications as the main peptide (peak 2 in MALDI & b in ESI) but missing the first 8 residues of the TEV-cleaved leader (GGSEFQTN, see Fig. S2). Peaks a & d in the ESI-MS spectrum are the $[M+4H]^{4+}$ and $[M+3H]^{3+}$ ions of the degradation product. Since this product appears in the GST-purified peptide sample, and results from cleavage of the peptide bond between two asparagines (N8 and N9, see Fig. S2B), which are susceptible to acid-catalyzed cleavage (10), we propose this results from TFA-catalyzed cleavage during workup. (*D*) Expanded windows of ESI mass spectrometry data for samples from 16 h cultures: TclK R181A (*top, left*), TclK R181A ΔTclS (*bottom, left*); and from 8 h cultures: TclK R181A (*top, right*) and TclK R181 ΔTclS (*bottom, right*). The insets show isotopic peaks for peak b in each panel (same as in Fig 4B) labeled 1-10 with *m/z* values listed in the tables. The average mass of a 6-thiazole, decarboxylated peptide is 5206.7 and its $[M+4H]^{4+}$ ion is peak b. Peak c is an unknown contaminant observed in most every LCMS run from the various mutant strains that elutes over a large time window.

A

```
                                                              *  *  *
TclK  129 REAVLQSFECEYFKNGVAMSNRNILKNYYKYVVN-NNNKKSRMTQQSIKNYYNRMNLKPSPFSTF 192
4wd9   30 TQVIETVSKNKVFLEQLLLANPKLYDVMQKYNAGLLKKKRVKKLFESIYKYYKRSYLRSTPFGLF 94

                                         *
TclK  193 TTIEINIEDYIVSDNK---HS-YEVYSEYNETYYKIIELSLLELDALDNIKKIKLNSSISKTKDN 253
4wd9   95 SETSIGVFSK---SSQYKLMGKTTKGIRLDTQWLIRLVHKMEVD--FSKKLSFTRNNANYKFGDR 154

TclK  254 YHYINVEMTPKYMYYKEKEMILKENITINECIHII----KKECFNYSK-SMKSIEKN-------- 305
4wd9  155 VFQVYTINSS-----------------ELEEVNIKYTNVYQIISEFCENDYQKYEDICETVTLCY 202

TclK  306 --LGSKGVNTFLY-LLKNNFLYLSFGI----DDYEKDKINKLSDMIKTTQTQDLTIIKVIQNLDK 363
4wd9  203 GDEYRELSEQYLGSLIVNHYLISNLQKDLLSDFSWNTFLTKVEAIDEDK--------KYIIPLKK 259

                                                             *
TclK  364 LSHLLNQINNKPFTYKEALVENIYLHTIDLLNLIGKQDIINTIESGSIIYQNN-IDTQITFPKEK 427
4wd9  260 VQKFIQEYSEIEIGEGIEKLKEIYQEMSQI------------LENDNYIQIDLISDSEINFDVKQ 312

TclK  428 LEVSFETVDIIHSIFRLFDDNIIEKIFMKKFFEKNYNNT--VKFKDFSKHFNSVYNEKNWEMIKK 490
4wd9  313 KQQLEHLAEFLGNTTKS--VRRTYLDDYKDKFIEKYGVDQEVQITELFDSTFGIGAPYNYNHPRN 375

TclK  491 T-----TELQTIK-KLREEFFTYIKNKKINSKDINLDTQWLKKFISTFP-DYLDCWESFSMYFQY 548
4wd9  376 DFYESEPSTLYYSEEEREKYLSMYVEAVKNHNVINL--DDLESHYQKMDLEKKSELQGLELFLNL 438

                                   *
TclK  549 NK--EDNYYILNDIGP--GMGRHILRYTRNLDNKNL--KFFTDTYKKNISEIENSKKKKYADISS 607
4wd9  439 AKEYEKDIFILGDIVGNNNLGGASGRFSALSPELTSYHRTIVDSVER----ENENKEITSCEIVF 499

TclK  608 -T---LSLNINLKSCSLNTQINYPTNNNKNNYN---ISDLFVTQKNGVLILVDEKGTEIDVTPTG 665
4wd9  500 LPENIRHANVMHTSIMRRKVLPFFTSTSHNEVLLTNIYIGIDEK-EKFYARDISTQEVLKFYITS 563

TclK  666 FLFPALAPETYKMLCRFSFSNGVQVNLWDRYSSFIDCNEEHFPNIFINNVLIEREVFNEKASDLQ 730
4wd9  564 MYNKTLFSNELRFLYEISLDDKFGNLPWELIY----RDFDYIPRLVFDEIVISPAKWKIWGRDVN 624

TclK  731 LLLENNTYEMMDLNEYLSNKIGIKEPLEFFSKFTYDIDALINENIIPEDWIKLIKNSKLRKPQYY 795
4wd9  625 SKM--------TIRELIQS---KEIPKEFYIVNGD-------------------------NKVYL 653

TclK  796 NLNNYLDFKNFSNII----KSVDSEQYVKIQKVNPRLND---------SNEYIYDFYKE       841
4wd9  654 SQKNPLDMEILESAIKKSSKR---KDFIELQEYFEDE-NIINKGEKGRVADVVVPFIRT       708
```

B

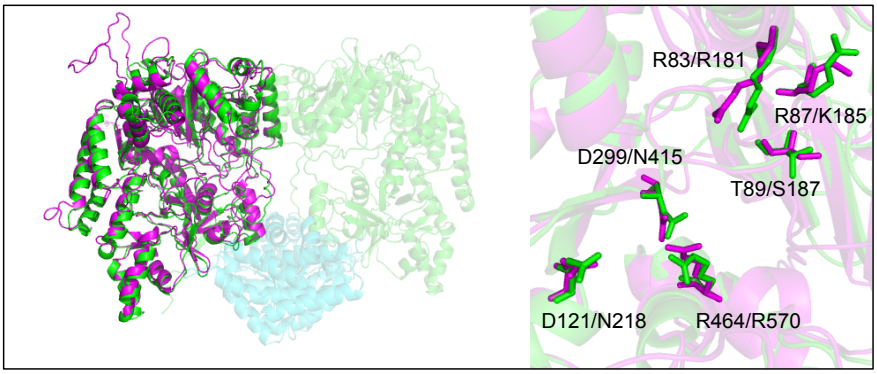

C

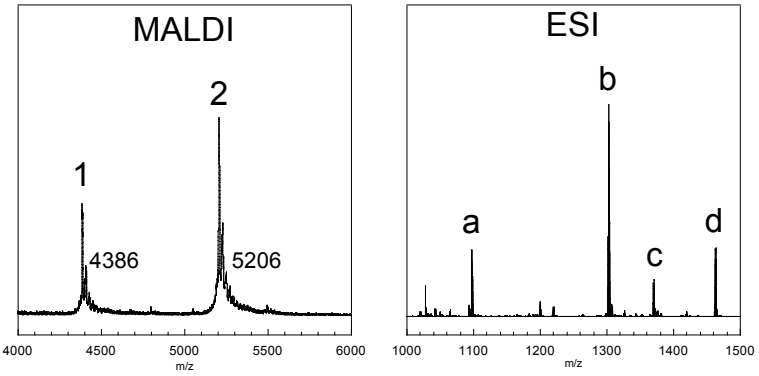

D

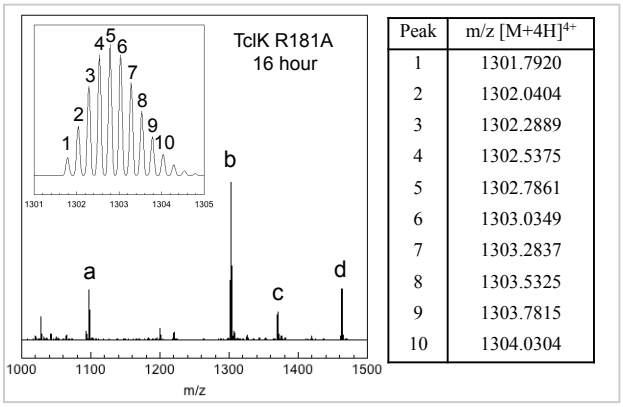

Peak	m/z [M+4H]$^{4+}$
1	1301.7920
2	1302.0404
3	1302.2889
4	1302.5375
5	1302.7861
6	1303.0349
7	1303.2837
8	1303.5325
9	1303.7815
10	1304.0304

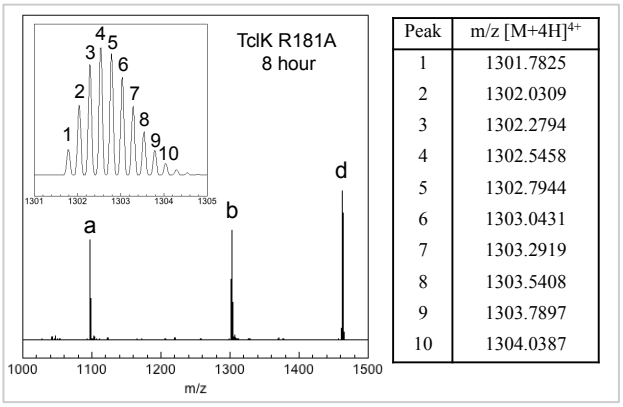

Peak	m/z [M+4H]$^{4+}$
1	1301.7825
2	1302.0309
3	1302.2794
4	1302.5458
5	1302.7944
6	1303.0431
7	1303.2919
8	1303.5408
9	1303.7897
10	1304.0387

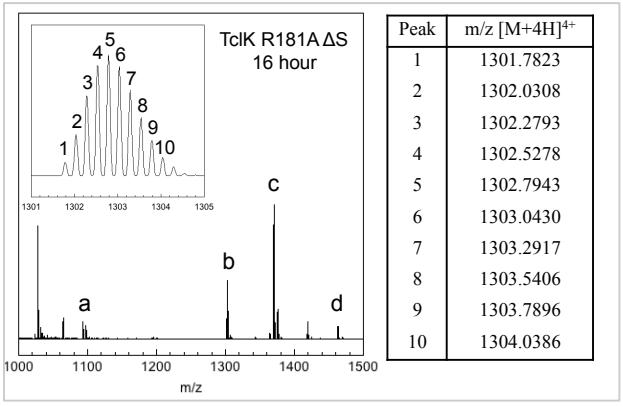

Peak	m/z [M+4H]$^{4+}$
1	1301.7823
2	1302.0308
3	1302.2793
4	1302.5278
5	1302.7943
6	1303.0430
7	1303.2917
8	1303.5406
9	1303.7896
10	1304.0386

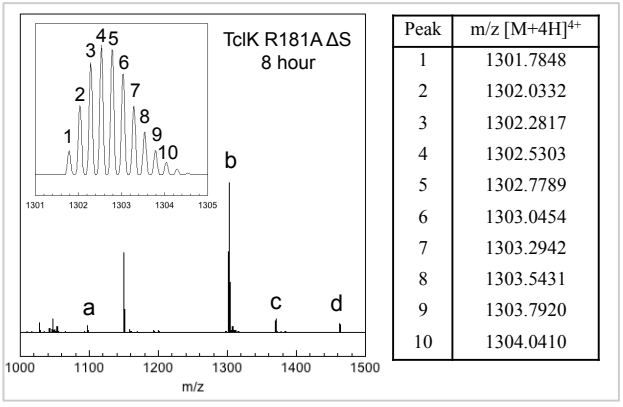

Peak	m/z [M+4H]$^{4+}$
1	1301.7848
2	1302.0332
3	1302.2817
4	1302.5303
5	1302.7789
6	1303.0454
7	1303.2942
8	1303.5431
9	1303.7920
10	1304.0410

Fig. S5. TclL structural modeling and expanded mass spectrometry data for modified TclE from the TclL-defective strains. (*A*) HHpred alignment of TclL with the C-terminal ~250 amino acids of NisB (PDB: 4WD9; probability >99%). Key residues identified in this domain of NisB as important for elimination of glutamic acid from glutamylated Ser and Thr residues to form dehydroalanines and dehydrobutyrines, respectively, are marked (*) (9, 11). A TclL R49A (*) mutation was used in this study to abolish enzyme activity resulting in the buildup of glutamylated peptide. (*B*) (*left & middle)* Overlay of the TclL structural model (Modeller) from the HHpred alignment (magenta) with the NisB dimer (green = N-term, cyan = C-term). (*right*) Close up showing alignment of key (*) residues (TclL – magenta, NisB – cyan). (*C*) MALDI-MS data for modified peptide from 16-h culture of TclL R49A mutant. (*inset*) Expanded view of lower intensity ion peaks: 2 Glu (*m/z* 5464, calc. *m/z* 5465.9), 3 Glu (*m/z* 5595, calc. *m/z* 5595.0), and 4 Glu (calc. *m/z* 5724.1, barely above the noise). (*D*) Comparison of MALDI-MS data for processed peptides from TclL R49A and ΔTclL strains. TEV-cleaved peptide from ΔTclL strain shows a simplified set of peaks, missing the lower (–18) *m/z* peak (*) that most likely arises from weak elimination activity of TclL R49A toward a single glutamylated Ser or Thr residue, which was also observed with the corresponding mutation in NisB (9). Data indicate TclL is not required to form a complex with TclK (or TclIJNP) since all other modifications are the same in the two strains. (*E*) ESI-MS data for peptides (0 Glu, 1Glu and 2 Glu) from 16-h cultures of TclL R49A, (*insets*) isotopic details of the major ion peak (*) in each. Obs. values refer to the average mass obtained from deconvoluting the envelope of isotopic peaks. Calc. values refer to the average mass of the 0, 1 and 2 Glu peptides containing a C-terminal ketone. (*F*) ESI-MS data for peptides from 8-h cultures of TclL R49A, (*insets*) isotopic details of the major ion peak (*) in each. Comparison of insets in (*E*) and (*F*) shows the shift from lower *m/z* at 8 h to higher *m/z* at 16 h for the most abundant isotope (*insets*, *) that arise from the slow, perhaps nonspecific, reduction of the C-terminal ketone to the alcohol.

A

```
TclL    1 MNWTSLHIFYFDN-NKELLVKCIYNMY--LNNFFDKFFYINYWDGGPH 45
4WD9  735 NEWLYLKLYISINRQNEFLLSYLPDIQKIVANLGGNLFFLRYTDPKPH 782
            * *
TclL   46 IRLRIANITKNEKEIIIKTIQKFIQENPSLSKISEKDYLITSNNFADK 93
4WD9  783 IRLRIKCS---DLFLAYGSILEILKRSRKN------------------- 809
                                    *
TclL   94 ENSEILELQKNNTILEIEYKPEIDKYLNNEGVHISEDIFFISSLNSLT 141
4WD9  810 --------RIMSTFDISIYDQEVERYGGFDTLELSEAIFCADSKIIPN 849

TclL  142 YLKNSPN---KEMVYMHSLQFANYILKY-F-LNTKQTVLFLKEYERYW 184
4WD9  850 LLTLIKDTNNDWKVDDVSILVNYLYLKCFFQNDNKKILNFLNLVSTKK 897

TclL  185 HSFSNSDIKSTKLI-RIPHK----KFA---------EFDDPFSKIKAN 218
4WD9  898 VK--------ENVNEKIEHYLKLLKVNNLGDQIFYDKNFKELKHAIKN 937
                                  *
TclL  219 -----FTHS-E-Q--MGFIFNYIHLTNNRL-GIKPFEEAILSSILTKF 256
4WD9  938 LFLKMIAQDFELQKVYSIIDSIIHVHNNRLIGIERDKEKLIYYTLQRL 985

TclL  257 WGDEYENKSNK                                     267
4WD9  986 FVSEEYMK---                                     993
```

B

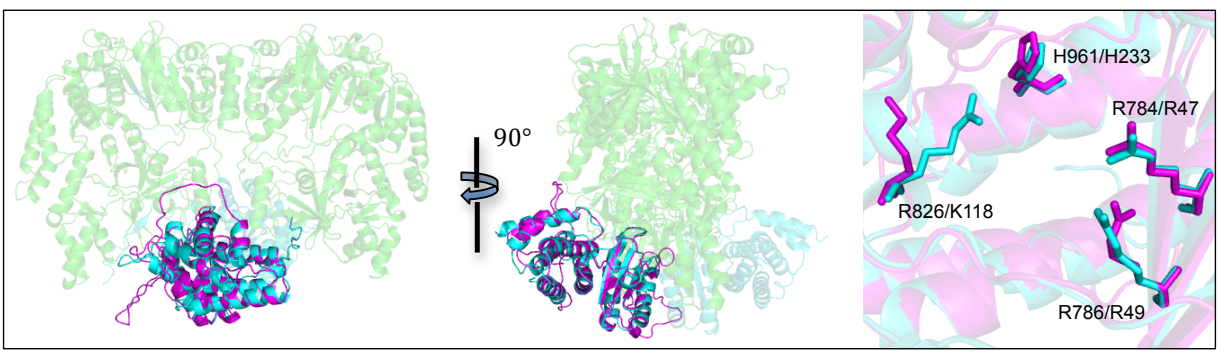

C

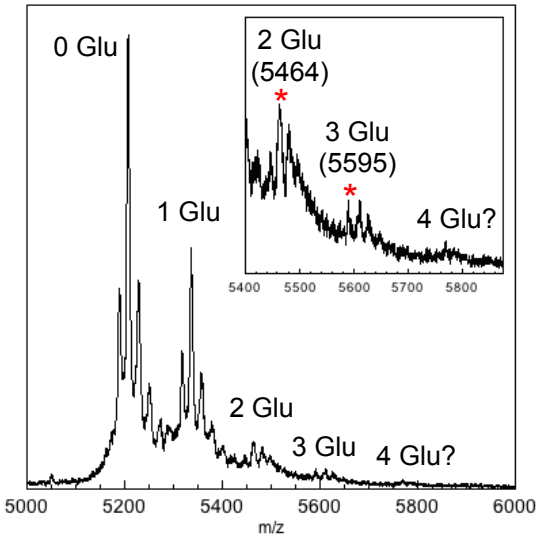
0 Glu
1 Glu
2 Glu
3 Glu
4 Glu?
2 Glu
(5464)
3 Glu
(5595)
4 Glu?
5400 5500 5600 5700 5800
5000 5200 5400 5600 5800 6000
m/z

D

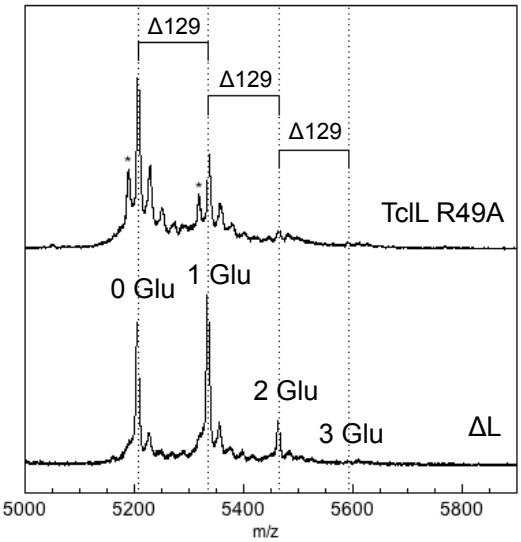
Δ129
Δ129
Δ129
TclL R49A
0 Glu
1 Glu
2 Glu
3 Glu
ΔL
5000 5200 5400 5600 5800
m/z

E

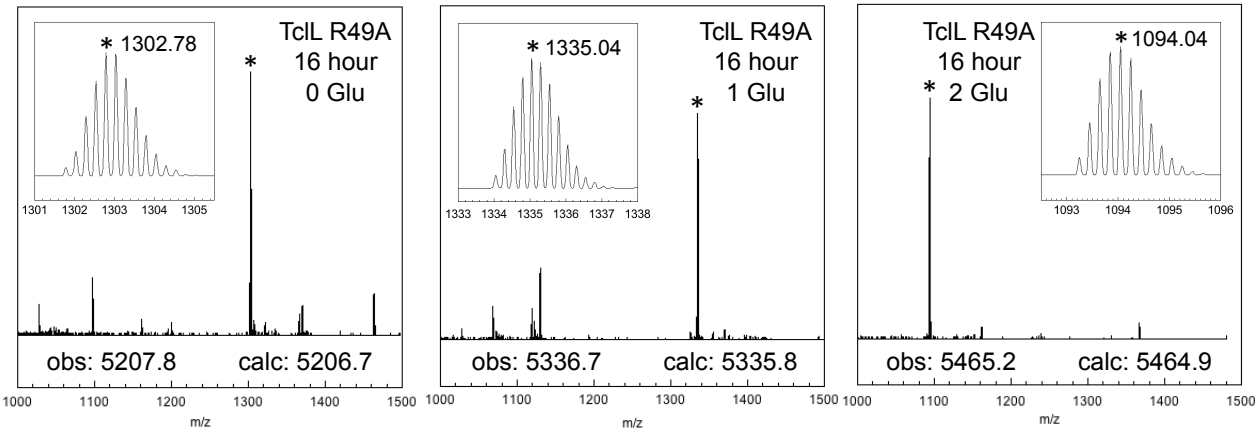
* 1302.78
TclL R49A
16 hour
0 Glu
1301 1302 1303 1304 1305
obs: 5207.8
calc: 5206.7
* 1335.04
TclL R49A
16 hour
1 Glu
1333 1334 1335 1336 1337 1338
obs: 5336.7
calc: 5335.8
TclL R49A
16 hour
* 2 Glu
* 1094.04
1093 1094 1095 1096
obs: 5465.2
calc: 5464.9
1000 1100 1200 1300 1400 1500
m/z

F

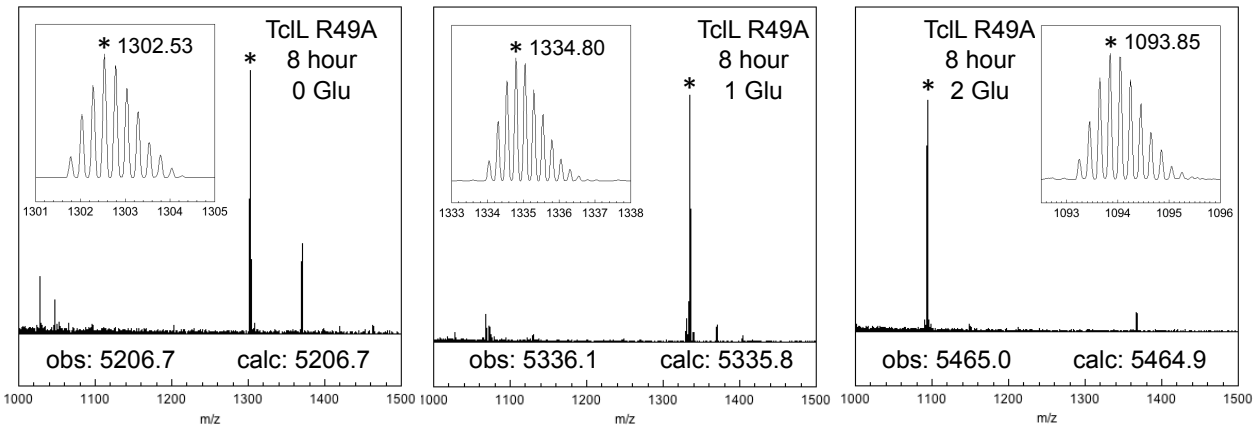
* 1302.53
TclL R49A
8 hour
0 Glu
1301 1302 1303 1304 1305
obs: 5206.7
calc: 5206.7
* 1334.80
TclL R49A
8 hour
1 Glu
1333 1334 1335 1336 1337 1338
obs: 5336.1
calc: 5335.8
TclL R49A
8 hour
* 2 Glu
* 1093.85
1093 1094 1095 1096
obs: 5465.0
calc: 5464.9
1000 1100 1200 1300 1400 1500
m/z

Fig. S6. TclN structural modeling and MALDI-MS data for modified TclE from the TclN-defective strain treated with formic acid or glutathione. (*A*) HHpred alignment of TclN with a putative nitroreductase from *Anabaena variabilis* ATCC 29413 (ava_2154, PDB: 3EO7, probability >99%). (*B, left*) Overlay of TclN model (Modeller, magenta) with structure of the single-FMN-containing putative nitroreductase (PDB: 3EO7, cyan). FMN is shown in green. (*B, right*) Close-up showing FMN binding site and key phosphate-binding residues in 3EO7 structure. An R269A/S271A (* in *A*) double mutant of the corresponding residues in TclN was made to disrupt FMN binding in order to inactivate the enzyme. (*C*) Comparison of MALDI-MS data for TclN R269A/S271A peptide from 16-h culture before (*top*) and after (*bottom*) incubation with 10% formic acid (>24 h) to rehydrate/ring-open the thiazolines. Incomplete conversion of peptide to a single peak with 0 dehydrations suggests small amounts of thiazole and Dha/Dhb are introduced over the longer culture time. (*D*) MALDI-MS data for TclN R269A/S271A peptide also show peaks consistent with glutathione (GSH ~Δ307) additions, suggesting small amounts of Dha/Dhb modifications are present in the sample (lower *m/z* set is from NN peptide cleavage) (12).

A

```
TclN    3 ISKFLYNLHYNPGEVVSASYTIEDTIQRNSEGFYKGYGIDFL-KLQQK 49
3EO7   10 AQHYHERTKYDPETIASKSQRLDWAKQPVPFKEYKIGSAIDLKPYLQ- 56

TclN   50 SPIVKVI----------LKSYGDIFFN--RVENKKK--PLIFCRKMTPS 84
3EO7   57 --ETPEVFVNDTNGQWWQRLSRLLFRSYGLTARMPSMGNTVYLRAAPS 102

TclN   85 GGGLYPINIFICTNF-KN-RIALFQFDFKRNLL-------------I-- 116
3EO7  103 AGGLYPAEVYVVSRGTPLLSPGLYNYQCRTHSLIHYWESDVWQSLQEA 150

TclN  117 --FIKYINIEINNECTK-LYLVPCYTRNYFKYKEFSYRLCPLDTGYLI 161
3EO7  151 CFWHPALES-----TQLAIIVTAVFYRSAWRYEDRAYRRICLDTGHLL 193

TclN  162 STLLYNFSVENITFKLSIKLNKNSDITDVLNEIGCEEIPYSIIELNE- 208
3EO7  194 GNIELSAAITDYRPHLIGGFID-EAVNDLLYIDPLQEGAIAVLPLADL 240

TclN      ------------------------------------------------
3EO7  241 LDIQQNISPGCTALPSATETNYPQVPDGELLKYFHHHTQISASITGKL 288

TclN  209 ----------SLNLDNLSLEHYDTESYFFNPNKVRNLLEIDTLIHQEY 246
3EO7  289 NLPTVIQEKSLEDKYNFPFCLKISTVS-APIYWGENLSDLEITMHK-- 333
                                        *  *
TclN  247 HKDININFNNENKLFEKFEIQKRISPGGEFIQNSKVEQESINKFISLI 294
3EO7  334 ----------------------RRST--RAYNGEELTFDELKALLDFT 357

TclN  295 MQYKNK-----SNFLSE--------YILLNLIDVQNKRIINLS--ASE 327
3EO7  358 YQPQNYIDQSLDNSPDYFDLNLIETFIAVCGVQGLEAGCYYYAPKAQE 405

TclN  328 FLSYKNNVSIEFIDKQLTRRNFNLLAVPYILYVGVNEEKIKENYSNNY 375
3EO7  406 LRQIRFKNFRREL-HFLCLGQELGRDAAAVIFHTSDLKSAIAQYGDRV 452

TclN  376 FKISRIIAGFWSGVVSILSAQCGLSTHPMMSYNARELEEYIF-KNRYS 422
3EO7  453 YRYLHMDAGHLGQRLNLAAIQLNLGVSGIGGFFDDQVNEVLGIPNDEA 500

TclN  423 ILNQIVIG                                        430
3EO7  501 VIYITTLG                                        508
```

B

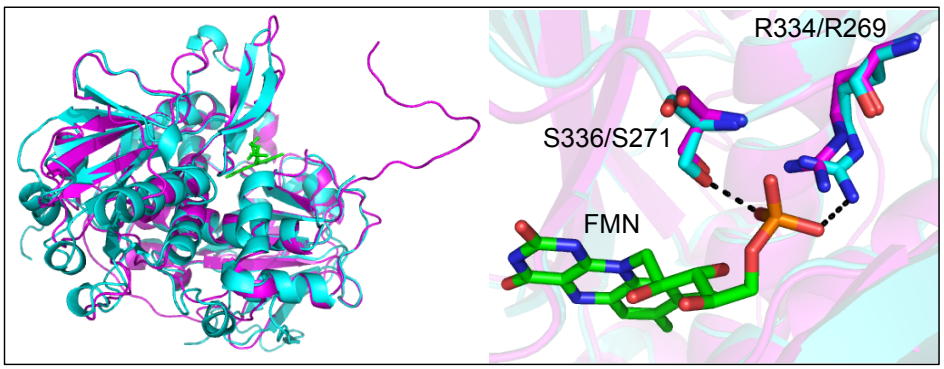
R334/R269
S336/S271
FMN

C

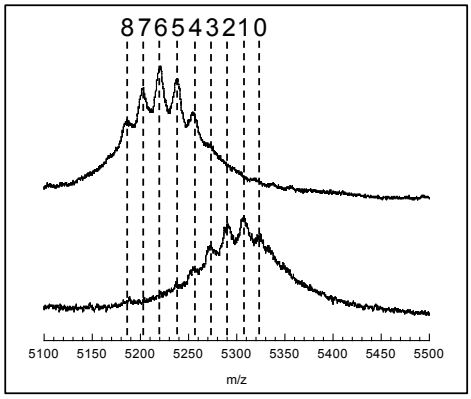
876543210
5100 5150 5200 5250 5300 5350 5400 5450 5500
m/z

D

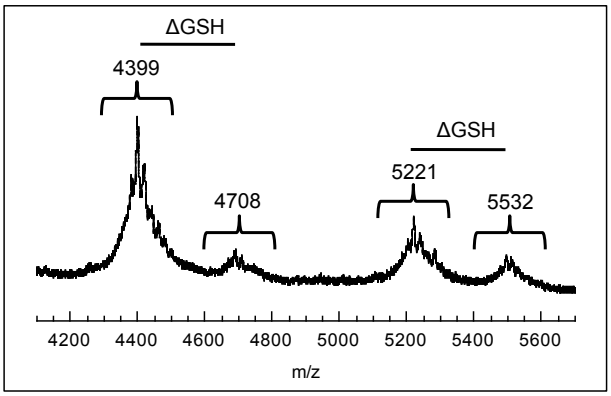
ΔGSH
4399
ΔGSH
5221
4708
5532
4200 4400 4600 4800 5000 5200 5400 5600
m/z

Fig. S7. TclP structural modeling, mutant bioassays, and expanded mass spectrometry data for modified TclE from the TclP-defective strains. (*A*) TclP is annotated as a short-chain dehydrogenase. It was aligned with (*R*)-hydroxypropyl-coenzyme M dehydrogenase (PDB: 2CFC) using HHpred (probability >99%). Three conserved active site residues shown to abolish activity in other short-chain dehydrogenases (13) were chosen for mutation: Asn97(*), S126(*) and Y139(*). (*B*) The methanol extract from TclP N97L showed no detectable bioactivity, however, extracts from TclP S126A and TclP Y139F retained activity. Extracts from cells expressing GST-TclE only or the full wild type pathway + GST-TclE are shown as negative and positive controls for bioactivity. (*C*) (*left*) Overlay of TclP model (magenta) (Modeller) with tetrameric (*R*)-hydroxypropyl-coenzyme M dehydrogenase (2CFC, cyan), NAD^+ is shown as green sticks. (*middle*) Close-up showing four conserved residues important for catalysis in other short-chain dehydrogenases (13-15). (*right*) Alternative orientation of active site, showing H-bonds from side chain of Asn114 (Asn97 in TclP) to backbone of Ile90 in 2CFC. (*D*) ESI mass spectrum of TEV-cleaved purified GST-peptide from TclP N97L mutant; major peak has *m/z* expected for peptide with an intact threonine at the C-terminus (i.e., no decarboxylation). Since no C-terminal processing has occurred, the isotopic pattern (*inset*) is consistent with a single product rather than a mix of alcohol and ketone as found for intermediates that have undergone decarboxylation. (*E*) MALDI-MS data for PP from ΔTclP (*top*) and TclP N97L (*bottom*) both show no oxidative decarboxylation activity as the major product is consistent with a peptide containing 6 thiazoles. Peaks consistent with minor amounts of 1-2 Ser/Thr dehydration are present (*) along with peaks for subsequent glutathione additions (#).

A

```
TclP    1 MNILIVGASSEIAHYIINYHK-IKDQVFLLDLPSQID-----N-LK-  39
2CFC    3 RVAIVTGASSGNGLAIATRFLARGDRVAALDLSAETLEETARTHWHA  49

TclP   40 KWD----TNFDTLDVQNNKEIETYFKECNITFDKLYYLVGINTM---  79
2CFC   50 YADKVLRVRADVADEGDVNAAIAATMEQFGAIDVLVNNAGITGNSEA  96
                                  *
TclP   80 KNGLDFNSQEWDNIMGTNLKSFYFFVKEFTKKNVINNI--PATIVSI 124
2CFC   97 GVLHTTPVEQFDKVMAVNVRGIFLGCRAVLPH---MLLQGAGVIVNI 140
          *                 *
TclP  125 ASQHGVVANAYRTPYCVSKAGLIHLTRVLALELSLYDIRVNCVSPGF 171
2CFC  141 ASVASLVAFPGRSAYTTSKGAVLQLTKSVAVDYAGSGIRCNAVCPGM 187

TclP  172 ILNSKSHEFLNNPKVKKEYLSKTPLQRYITPNEVANCCIFL--NNST 216
2CFC  188 IETPMTQWRLDQPELRDQVLARIPQKEIGTAAQVADAVMFLAGEDAT 234

TclP  217 SITGQNLIIDGGYTIW                                232
2CFC  235 YVNGAALVMDGAYTAI                                250
```

B

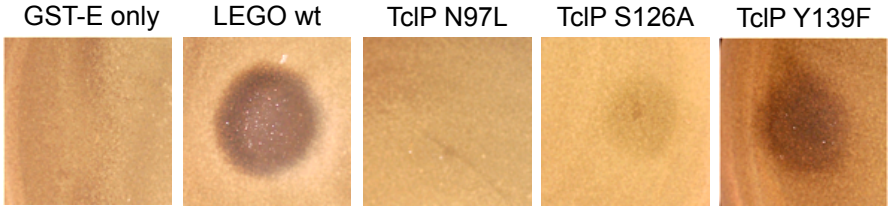

C

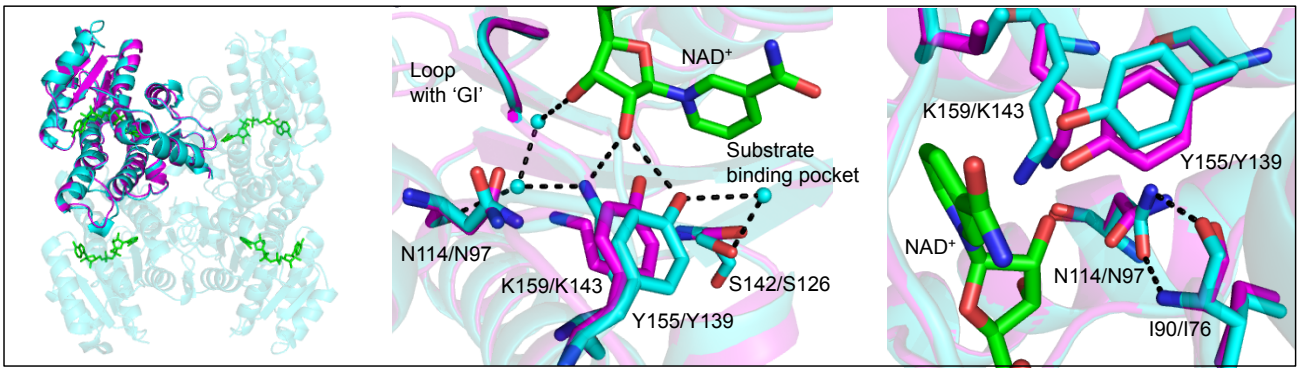
Loop
with 'GI'
NAD+
Substrate
binding pocket
N114/N97
K159/K143
S142/S126
Y155/Y139
K159/K143
Y155/Y139
NAD+
N114/N97
I90/I76

D

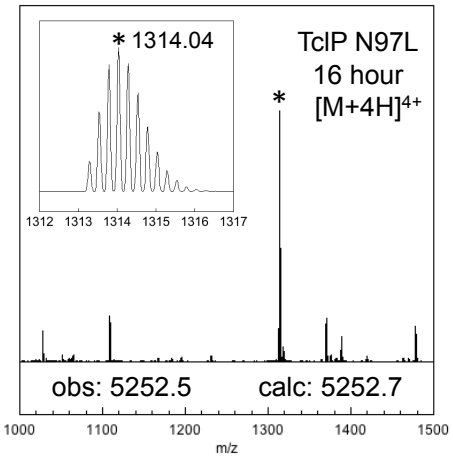
* 1314.04
1312 1313 1314 1315 1316 1317
TclP N97L
16 hour
[M+4H]4+
*
obs: 5252.5
calc: 5252.7
1000 1100 1200 1300 1400 1500
m/z

E

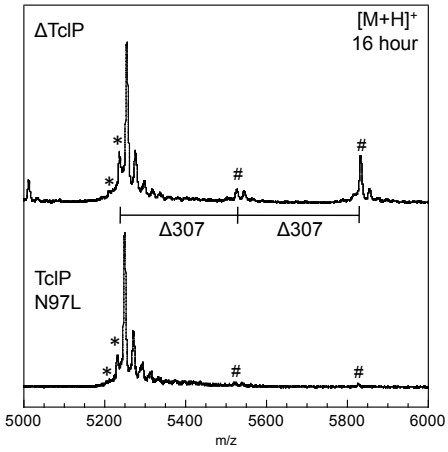
ΔTclP
[M+H]+
16 hour
*
*
#
#
Δ307
Δ307
TclP
N97L
*
*
#
#
5000 5200 5400 5600 5800 6000
m/z

Fig. S8. TclM alignments, mutant bioactivity assays, and mass spectrometry data for modified TclE from TclM-deletion strains. Currently no homologous crystal structures are available for structure modeling of TclM. (*A*) Clustal Omega sequence alignment of several TclM homologs from different thiopeptide clusters including McTclM: GenBank AIU53948.1, BcTclM: GenBank AAP11951.1, TbtD: GenBank ADG87279.1, LazC: GenBank BAO57436.1, BerD: GenBank AGN11669.1, NocO: GenBank ADR01090.1, NosO: GenBank ACR48344.1, GetF: GenBank AEM00619.1. Blue highlighting indicates sequence conservation (light = low, dark = high). Red (*) indicate amino acids that are the most important for catalytic activity in TbtD (16). (*B*) Bioassays of methanol extracts indicate mutations of two conserved residues, Y222A and R235A, in TclM did not abolish activity. Extracts from cells expressing GST-TclE only or the full wild type pathway + GST-TclE are shown as negative and positive controls for bioactivity. (*C*) Expanded window of ESI mass spectrometry data for TEV-cleaved peptides isolated from ΔTclM and ΔTclMΔTclS deletion mutants (same data as Fig. 4). (*D*) (*Left*) MALDI-MS data for TEV-cleaved peptide from a 16-h culture of ΔTclM mutant strain. The long culture resulted in cleavage of the (presumably processed) core peptide leaving just the leader peptide (`GGSEFQTNNIEGLDVTDLEFISEEVTEKDEKEIMGA`, expected *m/z* 3976 after TEV cleavage) attached to the GST-tag. (*Right & table*) MALDI-MS data for TEV-cleaved peptide obtained from an 8-h culture of the ΔTclM mutant strain that was eluted from the affinity resin with 10 mM reduced glutathione prior to TEV-cleavage. Peaks d-g are consistent with full length modified precursor with 0-3 additions of glutathione (Δ307 *m/z*) to the Dha/Dhb residues. Peaks a-c (*) are consistent with 1-3 GSH addition products of the NN cleavage product described in Fig. S4.

A

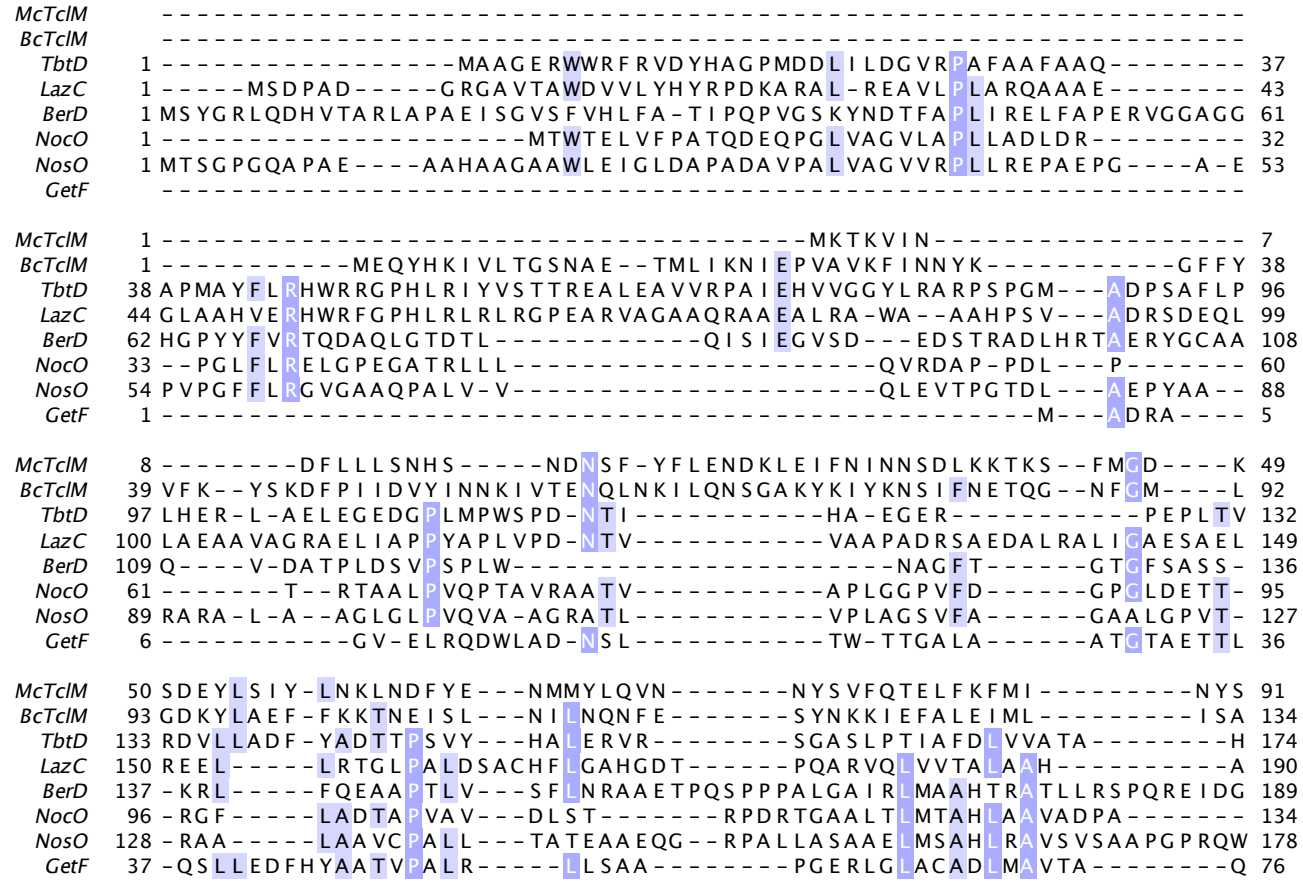

```
McTclM   92 EFNYESLERGMISYCSHSEGFLSIPK-NQKFKKIFKEGYLKNEHVLDLII-----NNRKDS- 146
BcTclM  135 HYNYDSIKKGYLSYASHVNGFFTRWKDPNKIRDIFHKNYLNNKEYLESKVSEIIDNNNRSS- 195
TbtD    175 ALSTGGLPVARTSLRSHAEAYLARRSDGVRLRELWRDHYARNREAFTERLIAVASSAESAEN 236
LazC    191 TAHPDGLVGAHYSVLSHLEDFLVHEDPDGSLRAAFERRWEQSGRAVTALVGRIADGGA---- 248
BerD    190 YEFRELLSLRLLSYRSHFEAIYLRTKDPQSFDAACARFYEQVGA----GVREFITACGDPDD 247
NocO    135 -RSGDGPPLSFLSFRSHAEAFLATTRDPNAARHAFDTRYTDHRTTVEAAVRAILLDGDPG-- 193
NosO    179 EELREGVPLGFLSYRSHAEAFLASSRDPKAAQAMMDAKYTRAAATLERLVDGVLTQCEERGP 240
GetF     77 EFGRGGLVSAALSFRSHAEAYLNLEAA-PDERAAWDAAARASAPALRRRLLAVATGPD---- 133

McTclM  147 ---FFYTYHIDTIISELKPCIRNSIKKNEIHFLNID----------HSKNN----DQLT 188
BcTclM  196 ------LSELSDIITEMKKEMTTDIEKGNLHVFNIE----------LLQKPGERDFLEK 238
TbtD    237 GAHLPHVREWVRRLRPIRERARALLESGELTLEY-A-SPA---------EGARDLP-SLAEV 286
LazC    249 ---RDWERDWAHWSATAWSLAERRLTAGADLGGRHAEYRERAEALGDPATAERWNAELRTRY 307
BerD    248 DPADEMVRLWTKSITSESSHLAENFSDGSVVNAGH--TLE---------DLVRKRG-APVEP 297
NocO    194 -----DAAPWSAAARAAKPRFTAGFASADLVAHT--GYTR---------DHLRERT-D-FAD 237
NosO    241 V-VSLPARQWYEAMRAAKPAVTELFRAGTDLALDTEEQPP---------DTGPDGK-G-LSE 290
GetF    134 --RPAYARDWLGLITPLVRAAEQAQRRGELALPT----------------LAEGFSS-DLTER 177

                                    *                   *
McTclM  189 SDFHQHMLSNEKFLKFMRCDIDFLTSRFLTIAQYFLLKNMGISNINRYFTCYLTYKSLSNFT 250
BcTclM  239 SQFHKTILNNPDFSNFMNKDINFLGSRLITVFTYLLIRNLGIQNKDRYLLCYYIYKIIEEKY 300
TbtD    287 SAFHRELESRPEWAR-LRDSPAFGAYRLVINCTYLHLTRLGLTPHQRFLVCHLAADAAADVY 347
LazC    308 SEFHRMLQRADPDGR-MWHRPDYLINRAGTNGLYRLLAICDVRPMERYLAAHLLVRSVPELT 368
BerD    298 TRFH--TPPSPELDRLMHRDADFLAFRLQTSLLYSCLYTLGFSLAERYVFCYVVARANEDVC 357
NocO    238 NPFHSRAGASEQLQAYLGGDPSFLATRLLTSLLYVTLHSSGVSLMQRYFLCHAIAKACESIY 299
NosO    291 SAFHRIVEGSDGLRDFLDRDPSFLATRLLTSLLYLSLSSVGIALAERYFLCYAVSRACESIF 352
GetF    178 SAFHRGLAGSTSWED-VRTSDWFVLYRFAINLLYLQLSRLGVKPVGRYRLCHLVATALDQRE 238

McTclM  251 SKNPNDLIKYFKED---------------------------- 264
BcTclM  301 NIDTLELIRDFGKGRD---NNVEDL-----QRY-------- 325
TbtD    348 GIAAHEEVAT---R---------------------------- 358
LazC    369 GHRWQTLLGAAEQPGGPEQSGAAGATGGAGRTKLEGAA 406
BerD    358 GKSMKELQDELDGLAR---SMASGSTKTAE--------- 384
NocO    300 HVDSMSLLAD---LAV---G------------------- 313
NosO    353 DTDALTVLSG---LAR---TSLAS--------------- 370
GetF    239 APTTTAEEGD---S------------------------- 249
```

B

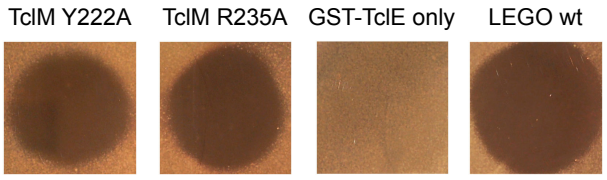

C

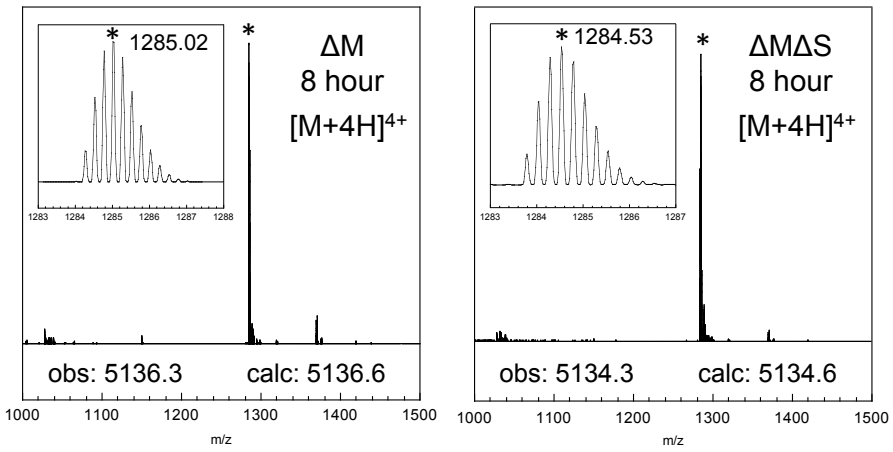

D

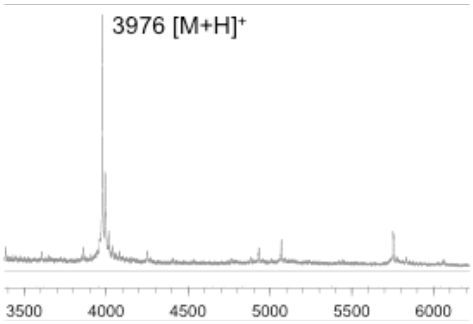

m/z

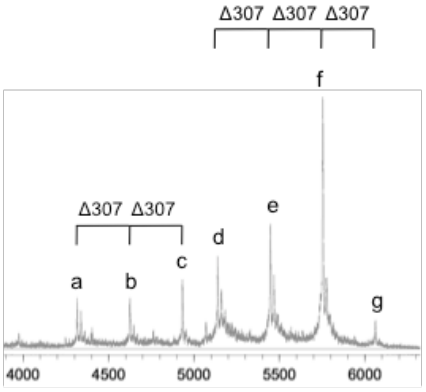

m/z

peak	$[M+H]^+$	# of GSH adducts
a	4319*	1
b	4626*	2
c	4932*	3
d	5138	0
e	5447	1
f	5754	2
g	6062	3

Table S1. Plasmids used to generate *tcl* mutant strains.

Plasmid	Genotype[a]	Description[b]
pLEGO	P_{xyl}-TclIJKLMNPS	Parental plasmid containing all MP1 processing genes. Used as template DNA for generating all mutant constructs.
L7152D7	TclJ E319A	TclJ E319A was amplified from pLEGO by OE-PCR using oPB465 as external forward primer, oPB471 as internal reverse primer, oPB470 as internal forward primer and oPB474 as external reverse primer
L7153C5	TclK R181A	TclK R181A was amplified from pLEGO by OE-PCR using oPB475 as external forward primer, oPB478 as internal reverse primer, oPB477 as internal forward primer and oPB476 as external reverse primer
L7154C1	TclL R49A	TclL R49A was amplified from pLEGO by OE-PCR using oPB447 as external forward primer, oPB485 as internal reverse primer, oPB484 as internal forward primer and oPB483 as external reverse primer
L769A1	TclM Y222A	TclM Y222A was amplified from pLEGO by OE-PCR using oPB500 as external forward primer, oPB534 as internal reverse primer, oPB533 as internal forward primer and oPB011 as external reverse primer
L769B1	TclM R235A	TclM R235A was amplified from pLEGO by OE-PCR using oPB500 as external forward primer, oPB536 as internal reverse primer, oPB535 as internal forward primer and oPB011 as external reverse primer
L769C1	TclP N97L	TclP N97L was amplified by from pLEGO OE-PCR using oPB507 as external forward primer, oPB538 as internal reverse primer, oPB537 as internal forward primer and oPB506 as external reverse primer
L769D1	TclP S126A	TclP S126A was amplified from pLEGO by OE-PCR using oPB507 as external forward primer, oPB540 as internal reverse primer, oPB539 as internal forward primer and oPB506 as external reverse primer
L769E1	TclP Y139F	TclP Y139F was amplified from pLEGO by OE-PCR using oPB507 as external forward primer, oPB542 as internal reverse primer, oPB541 as internal forward primer and oPB506 as external reverse primer
L783A1	TclN R269A/S271A	TclN R269A/S271A was amplified from pLEGO by OE-PCR using oPB448 as external forward primer, oPB549 as internal reverse primer, oPB550 as internal forward primer and oPB503 as external reverse primer
L762A1	ΔTclM	pLEGOΔTclM was constructed by treating pLEGO with SacI/SalI/Klenow and religating plasmid
L762D1	ΔTclS	pLEGOΔTclS was constructed by treating pLEGO with XhoI/BglII/Klenow and religating plasmid
L783G2	ΔTclL	pLEGOΔTclL was constructed by treating pLEGO with PstI/SacI/Klenow and religating plasmid
L794C2	ΔTclM,ΔTclS	pLEGOΔTclMS was contructed by treating pLEGOΔTclM (L762A1) with XhoI/BglII/Klenow and religated

[a] Genotypes represent variations in pLEGO, which integrate into the *amyE* locus of *B. subtilis*; [b] Full primer sequences are provided in Table S2. OE-PCR: overlap extension polymerase chain reaction.

Table S2. Primers used in this study.

Primer	Sequence (5'-3')
oPB281	CCGCCTTGAAAATACAGGTTTTCTCCTCCTTTTGGAGGATGGTCGC
oPB282	CCTGTATTTTCAAGGCGGATCAGAATTCCAAACAAACAAT
oPB288	GCGTCTAGAAAGGaGGtgGAGGTCATGTCCCCTATACTAGGTTA
oPB289	CGCGGATCCTTAAGTTGTACAACAACTGCA
oPB011	GCTGACACAACTTCTCCTGG
oPB447	GTGAATCCTCGTCTTAATGATTCA
oPB448	CTCTATCCAATTTCACATCTAAAAATCC
oPB465	CAAGTTTAATGTCCAAACTTTTGAAGGTG
oPB470	GTATATTATGGCCTAATGGCAGTTATCGAGAGAGACTCTT
oPB471	AAGAGTCTCTCTCGATAACTGCCATTAGGCCATAATATAC
oPB474	CTGTTACATTTACGCGTTATACTATAAGGC
oPB475	GTACCTGGATTATTACCTATGACTTTCGG
oPB476	AAGATATGTAGGCTTGTCCAATTCA
oPB477	CCATAAAAAATTACTACAATGCAATGAATTTAAAACCTTCTC
oPB478	GAGAAGGTTTTAAATTCATTGCATTGTAGTAATTTTTTATGG
oPB483	GATAAGTATTCGTCACTTTTATCACCC
oPB484	GGTCCTCATATCCGTCTAGCAATAGCTAATATTACAAAGA
oPB485	TCTTTGTAATATTAGCTATTGCTAGACGGATATGAGGACC
oPB500	CGAACAATAGATTAGGAATCAAACC
oPB503	CTATCTGAGAAGGAAGATCAAGTAG
oPB506	GTAAAGCAATAGGACTTGTTCCTCC
oPB507	GGTCTATCTACCCACCCAATGATG
oPB533	TTTCTTACAATAGCTCAAGCCTTTTTATTAAAAAACATGG
oPB534	CCATGTTTTTTAATAAAAAGGCTTGAGCTATTGTAAGAAA
oPB535	CATGGGAATAAGTAATATTAACGCATATTTCACTTGCTAT
oPB536	ATAGCAAGTGAAATATGCGTTAATATTACTTATTCCCATG
oPB537	GACAATATAATGGGGACTCTTCTCAAAAGCTTTTATTTC
oPB538	GAAATAAAAGCTTTTGAGAAGAGTCCCCATTATATTGTC
oPB539	CCATAGTTAGTATTGCAGCTCAACATGGCGTC
oPB540	GACGCCATGTTGAGCTGCAATACTAACTATGG
oPB541	CTAATGCCTATAGAACTCCTTTTTGTGTAAGTAAAGCTGG
oPB542	CCAGCTTTACTTACACAAAAAGGAGTTCTATAGGCATTAG
oPB549	AAATTCGCCACCCGGAGCTATTGCTTTTTGTATTTCGAAT
oPB550	ATTCGAAATACAAAAAGCAATAGCTCCGGGTGGCGAATTT

SI References

1. Bennallack PR, Burt SR, Heder MJ, Robison RA, & Griffitts JS (2014) Characterization of a novel plasmid-borne thiopeptide gene cluster in *Staphylococcus epidermidis* strain 115. *J Bacteriol* 196(24):4344-4350.
2. Waterhouse AM, Procter JB, Martin DMA, Clamp M, & Barton GJ (2009) Jalview Version 2—a multiple sequence alignment editor and analysis workbench. *Bioinformatics* 25(9):1189-1191.
3. Pettersen EF*, et al.* (2004) UCSF Chimera—A visualization system for exploratory research and analysis. *J Comput Chem* 25(13):1605-1612.
4. Sievers F*, et al.* (2011) Fast, scalable generation of high‐quality protein multiple sequence alignments using Clustal Omega. *Mol Syst Biol* 7(1):article 539.
5. Zhang Z & Marshall AG (1998) A universal algorithm for fast and automated charge state deconvolution of electrospray mass-to-charge ratio spectra. *J Am Soc Mass Spectrom* 9(3):225-233.
6. Bennallack PR*, et al.* (2016) Reconstitution and minimization of a micrococcin biosynthetic pathway in *Bacillus subtilis*. *J Bacteriol* 198(18):2431-2438.
7. Koehnke J*, et al.* (2015) Structural analysis of leader peptide binding enables leader-free cyanobactin processing. *Nat Chem Biol* 11(8):558-563.
8. Dunbar KL*, et al.* (2014) Discovery of a new ATP-binding motif involved in peptidic azoline biosynthesis. *Nat Chem Biol* 10(10):823-829.
9. Garg N, Salazar-Ocampo LMA, & van der Donk WA (2013) In vitro activity of the nisin dehydratase NisB. *Proc Natl Acad Sci USA* 110(18):7258-7263.
10. Rawlings ND, Barrett AJ, & Bateman A (2011) Asparagine peptide lyases: a seventh catalytic type of proteolytic enzymes. *J Biol Chem* 286(44):38321-38328.
11. Ortega MA*, et al.* (2015) Structure and mechanism of the tRNA-dependent lantibiotic dehydratase NisB. *Nature* 517(7535):509-512.
12. Rose NL*, et al.* (2003) Involvement of dehydroalanine and dehydrobutyrine in the addition of glutathione to nisin. *J Agric Food Chem* 51(10):3174-3178.
13. Filling C*, et al.* (2002) Critical residues for structure and catalysis in short-chain dehydrogenases/reductases. *J Biol Chem* 277(28):25677-25684.
14. Krishnakumar AM, Nocek BP, Clark DD, Ensign SA, & Peters JW (2006) Structural basis for stereoselectivity in the (R)- and (S)-hydroxypropylthioethanesulfonate dehydrogenases. *Biochemistry* 45(29):8831-8840.
15. Sliwa DA, Krishnakumar AM, Peters JW, & Ensign SA (2010) Molecular basis for enantioselectivity in the (R)- and (S)-hydroxypropylthioethanesulfonate dehydrogenases, a unique pair of stereoselective short-chain dehydrogenases/reductases involved in aliphatic epoxide carboxylation. *Biochemistry* 49(16):3487-3498.
16. Hudson GA, Zhang Z, Tietz JI, Mitchell DA, & van der Donk WA (2015) In vitro biosynthesis of the core scaffold of the thiopeptide thiomuracin. *J Am Chem Soc* 137(51):16012-16015.